

# Approximate normalizations for approximate density functionals

Adam Clay<sup>1</sup>, Kiril Datchev<sup>1</sup>, Wenlan Miao<sup>2</sup>, Adam Wasserman<sup>2,3</sup>, Kimberly J. Daas<sup>4</sup>, and Kieron Burke<sup>4,5</sup>

<sup>1</sup>*Department of Mathematics, Purdue University, West Lafayette, IN 47907, USA*

<sup>2</sup>*Department of Physics and Astronomy, Purdue University, West Lafayette, IN 47907, USA*

<sup>3</sup>*Department of Chemistry, Purdue University, West Lafayette, IN 47907, USA*

<sup>4</sup>*Department of Chemistry, University of California, Irvine, CA 92697, USA and*

<sup>5</sup>*Department of Physics and Astronomy, University of California, Irvine, CA 92697, USA*

It seems self-evident that a density functional calculation should be normalized to the number of electrons in the system. We present multiple examples where the accuracy of the approximate energy is improved (sometimes greatly) by violating this basic principle. In one dimension, we explicitly derive the appropriate correction to the normalization. Beyond one dimension, Weyl asymptotics for energy levels yield these corrections for any cavity. We include examples with Coulomb potentials and the exchange energy of atoms to illustrate relevance to realistic calculations.

It is a truth universally acknowledged, that any density functional calculation should yield a density that integrates to the number of electrons in the system. No matter how little is known about the functionals involved, this truth is so well fixed in the minds of practitioners that the normalization step passes almost unnoticed [1].

Sophisticated approximations to the exchange-correlation functional of Kohn–Sham DFT [2, 3], together with improved algorithms and powerful computers, allow for efficient and accurate calculations on systems with thousands of atoms [4]. With advances in quantum embedding methods [5] and orbital-free DFT [6], even millions of atoms can be treated [7], with applications ranging from molecular biology [8] to drug design [9] and materials engineering [10]. But in the sixty years since the foundational papers, it has never been questioned that, even when minimizing an approximate energy functional, the best normalization constraint is to require that  $\int d\mathbf{r} n(\mathbf{r}) = N$ , i.e. the density integrates to the number of electrons in the system. However, motivated by recent advances in the semiclassical study of DFT [11, 12], we show here that an approximate normalization  $\int d\mathbf{r} n(\mathbf{r}) = \tilde{N} = N + \Delta N$ , derived from asymptotic considerations, yields much better energetics than the usual norm. Remarkably, it often yields better results than the same functional evaluated on the exact density (the basic idea behind density-corrected DFT improvements [13–16]). This also represents the generalization of many semiclassical DFT results beyond one dimension. [12, 17–20]

We start with a simple example:  $N$  noninteracting, spinless electrons in one dimension [21]. The local density approximation for such problems is the Thomas-Fermi approximation for the kinetic energy [22, 23], here  $\pi^2 \int dx n^3(x)/6$  (using Hartree atomic units). For the simplest case, the infamous particle(s)-in-a-box, with  $v = 0$  and  $L = 1$ , Fig. 1 compares three approximations for the energy  $E(N)$ . The first is the standard DFT treatment, where  $n(x)$  is found by minimizing the functional, so  $n(x) = N$ . This energy is denoted  $\tilde{E}(N)$ , and

shown in red in the top panel, with its density in the bottom. The TF functional evaluated on the exact density (green), with energy  $\tilde{E}_d(N)$ . The blue is normalization-corrected TF,

$$\tilde{E}_{\text{nc}}(N) = \tilde{E}(\tilde{N}), \quad \tilde{N} = N + \Delta N. \quad (1)$$

where  $\Delta N = 1/2$ , outperforms in all cases. Energy expressions can be found in Section S1 of the Supplemental Material. The normalization correction makes the approximate density closer to the true density away from the walls, an idea that dates back to Scott [24].

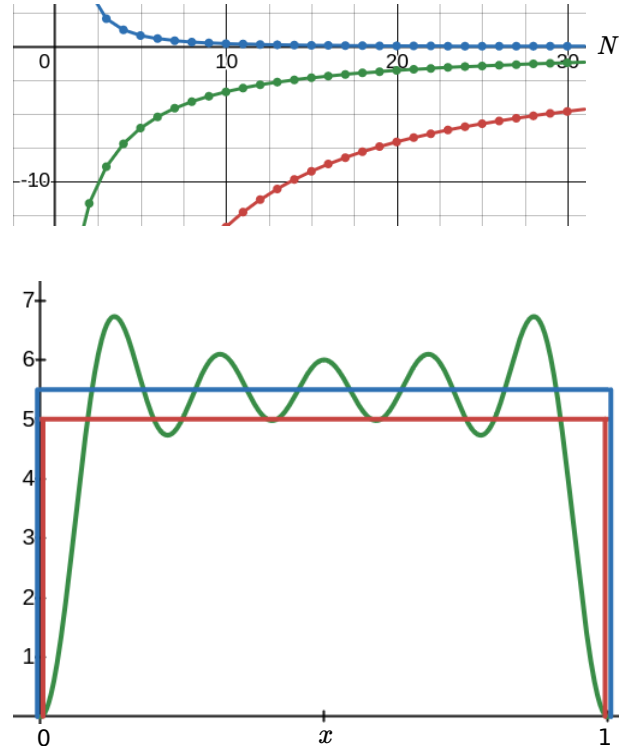


FIG. 1. *Bottom:* Red is the TF density, green the exact density, and blue the normalization-corrected density for  $N = 5$ . *Top:* Percent errors for the TF energy evaluated on each density (See Table S1).

In this first example, the correction  $\Delta N$  can be derived from the explicit formula for the density  $n(x) = \tilde{N} - r(x)$ ,  $r(x) = \sin(2\tilde{N}\pi x)/2\sin(\pi x)$  is a lower order term on average, away from the walls. Ignoring the density oscillations yields a better energy than accounting for them and has the advantage of staying within the family of densities belonging to the TF functional. In mathematical terms, the TF densities of differing  $N$  form a *foliation* of the graph space [25]. For a box or cavity, TF densities are constants and our correction yields the constant which best approximates the bulk, at the expense of the edge. Our approximate constraint beats the exact constraint and even beats using the exact density.

This paper presents a proof of principle for our method, focusing on the non-interacting TF kinetic energy functional [22, 23], which was first mathematically analyzed in [26, 27]. We first derive and generalize the 1D example above, using WKB theory [28]. We next explain how Weyl asymptotics for energy levels in cavities can be used to derive values of  $\Delta N$  in higher dimensions, with various examples; for instance, Fig. 2 is the analog of the bottom panel of Fig. 1 for a 2D circular cavity (see also [29]). We also give several examples for specific simple potentials, ending with interacting systems and the exchange energy, to connect to realistic DFT calculations.

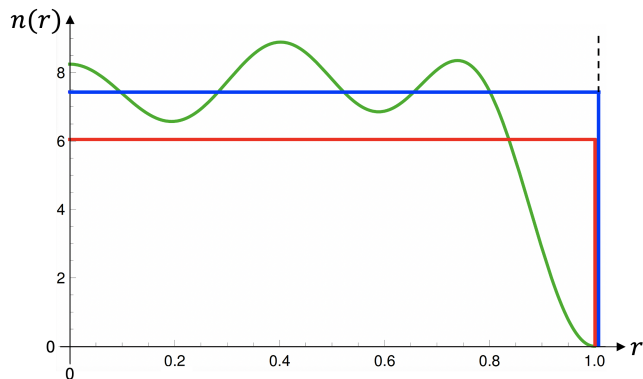


FIG. 2. Densities for 19 electrons (11 filled shells) in a circular cavity of radius 1. Green is the exact density, red is TF, and blue is ncTF (Sec. S7). An analogous phenomenon, also derived from Weyl asymptotics, is observed in [29, Fig. 2].

*One dimension:* For the Hamiltonian  $-(1/2)d^2/dx^2 + v(x)$ , the TF and WKB approximations are essentially equivalent [30]. From WKB [31, (1.308)], under reasonable conditions on  $v(x)$  [32], we have an implicit formula for individual energy levels

$$\int_{-\infty}^{\infty} \frac{dx}{\pi} p(\mathcal{E}, x) = \lambda(j) := j - \nu + r(j), \quad (2)$$

where  $p(\mathcal{E}, x) = \sqrt{2(\mathcal{E} - v(x))_+}$  is the classical momentum,  $j$  is a positive integer,  $\nu$  is the Maslov index [33] (0 if there are only hard walls, and increases by 1/4 for each classical turning point), and  $r(j)$  is a remainder which

vanishes at least as fast as  $j^{-1}$ . The exact levels are

$$\mathcal{E}_j = \mathcal{E}(\lambda(j)) = \mathcal{E}(j - \nu + r(j)),$$

where  $\mathcal{E}(\lambda)$  solves Eq. (2). Summing over  $N$  levels yields, for the dominant behavior as  $N \rightarrow \infty$ ,

$$E(N) = \sum_{j=1}^N \mathcal{E}_j \sim \int_0^N d\lambda \mathcal{E}(\lambda). \quad (3)$$

By changing variables  $\lambda \rightarrow \mathcal{E}$ , differentiating (2), and swapping the order of integration, [30] showed that  $\int_0^N d\lambda \mathcal{E}(\lambda) = \tilde{E}(N)$ , precisely [34].

An exact version of (3), similar to [35], is

$$E(N) = \int_{1/2}^{N+1/2} d\alpha \left( \mathcal{E}(\lambda(\alpha)) + s(\alpha) \frac{d}{d\alpha} \mathcal{E}(\lambda(\alpha)) \right), \quad (4)$$

where  $s(\lambda) = \lambda - \lfloor \lambda \rfloor - 1/2$  is a saw-tooth function, and we have extended  $\lambda(\alpha)$  from (2) smoothly to noninteger  $\alpha$ . To check (4), integrate by parts in the second term, and simplify. Assuming certain derivatives of  $\mathcal{E}(\lambda)$  and  $r(\alpha)$  are well-behaved, from (4) the leading correction to (3) is

$$E(N) \sim \int_0^{N+1/2-\nu} d\lambda \mathcal{E}(\lambda) = \tilde{E}(N + 1/2 - \nu). \quad (5)$$

This yields  $\Delta N = 1/2 - \nu$ , so  $\Delta N = 1/2$  in the two-wall case of the introduction (first row of Table III) and  $\Delta N = 1/4$  in the one-wall case (second and third rows of Table III). For a harmonic oscillator,  $\mathcal{E}(\lambda) = \omega\lambda$ ,  $\nu = 1/2$ , for a particle in a box,  $\mathcal{E}(\lambda) = \pi^2\lambda^2/2L^2$ ,  $\nu = 0$ , and for a linear half well  $\mathcal{E}(\lambda) = (3\pi\lambda/2)^{2/3}$ ,  $\nu = 1/4$ .

*Weyl asymptotics:* In higher dimensions, Weyl asymptotics [36, 37] provide precise information about energy levels for many Hamiltonians, including general classes of potentials and cavities [38]. To derive a good  $\Delta N$  from such asymptotics is simple. We begin with  $N$  noninteracting, spinless electrons in a  $d$ -dimensional cavity. Weyl asymptotics state that

$$E(N) = C_1 N^{1+2/d} + C_2 N^{1+1/d} + \dots, \quad (6)$$

where  $C_1$  and  $C_2$  depend on the geometry of the cavity in a simple, explicit way [39, Eq. (6)]; see also [29]. Related asymptotics hold for other Hamiltonians [38, 40]. The TF approximation yields precisely the first term only, and we choose  $\tilde{N}$  to recover the second as  $N \rightarrow \infty$ . Thus,  $\tilde{E}(N)$  corresponds to a one-term Weyl asymptotic and  $\tilde{E}_{\text{nc}}(N) = \tilde{E}(\tilde{N})$  to a two-term Weyl asymptotic. Table I and Fig. 3 show the accuracy of  $\tilde{E}_{\text{nc}}(N)$  for a 3D box.

Originally, Weyl asymptotics were conjectured over a century ago in [37] and proved in [41, 42] and these come from problems in acoustics and black-body radiation, and are important throughout mathematics and physics [40].

$N$	$E(N)$	$\tilde{E}(N)$	$\tilde{E}_d(N)$	$\tilde{E}_{nc}(N) = \tilde{E}(\tilde{N})$
1	7.90	1.69 (-79%)	3.61 (-54%)	5.38 (-32%)
10	161	78.3 (-51%)	120 (-26%)	148 (-8%)
100	5141	3633 (-29%)	4490 (-13%)	5039 (-2%)
1000	198838	168647 (-15%)	187810 (-6%)	197873 (-0.5%)

TABLE I. Exact and approximate energy values for a 3D box with incommensurate edges  $1 \times \sqrt{2} \times \pi$ . See Fig. 3 and Sec. S3

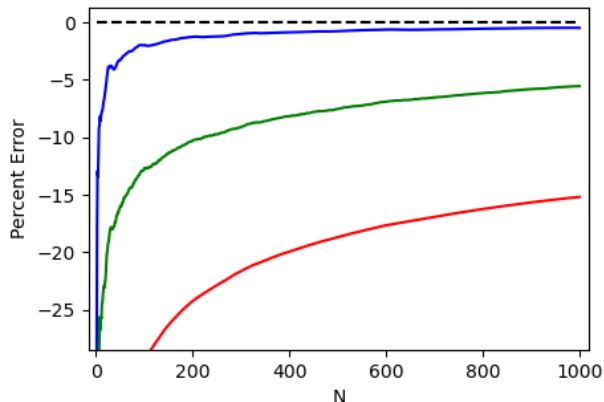


FIG. 3. Red is energy-minimized TF, green is TF on the exact density, and blue is normalization-corrected TF, for a  $1 \times \sqrt{2} \times \pi$  box.

The relevant quantities are averaged versions of the traditional asymptotics, which have been recently proven for very general cavities [43–46].

*Generality:* Table III presents further and richer examples of our method. In all cases, we find

$$\tilde{E}(N) = AN^p, \quad \Delta N = BN^q \quad (7)$$

A key feature is that the formula for the correction power  $q$ , unlike those for  $p$ ,  $A$ , or  $B$ , is universal. Moreover, the sign of  $B$  follows that of divergences in the potential, intuitively matching the error in the TF density in the interior. Fig. 4 shows the significance of the normalization correction across cavities of different shapes.  $B$  increases with aspect ratio, so TF correspondingly loses accuracy, while ncTF remains accurate even for very elongated boxes. The formula  $\Delta N = (|\partial\Omega|/3\sqrt{|\Omega|\pi})N^{1/2}$  works for 2D cavities of any shape. Table II lists results for a circular cavity, where  $\Delta N = (2/3)N^{1/2}$ .

Generally, the more accurate an approximate energy functional is, the smaller  $\Delta N$  is, but a good choice of  $\Delta N$  improves energies ( $\Delta N$  vanishes for the 1D harmonic oscillator because of perfect cancellation of errors in TF). Typically  $\Delta N$  is small when the potential is smooth. For the two-dimensional isotropic harmonic oscillator  $\Delta N = 1/24$  when all shells are filled, while the exact energy is

$$E(N) = \frac{\omega}{3}N\sqrt{8N+1}. \quad (8)$$

$N$	$E(N)$	$\tilde{E}(N)$	$\tilde{E}_{nc}(N) = \tilde{E}(\tilde{N})$
19	487	361 (-26%)	480 (-2%)
30	1139	900 (-21.0%)	1132 (-0.6%)
100	11,408	10,000 (-12%)	11,378 (-0.3%)
1000	1,042,850	1,000,000 (-4%)	1,042,608 (-0.02%)

TABLE II. Exact and approximate energy values for a circular cavity of radius one. (Energy expressions in Sec. S7)

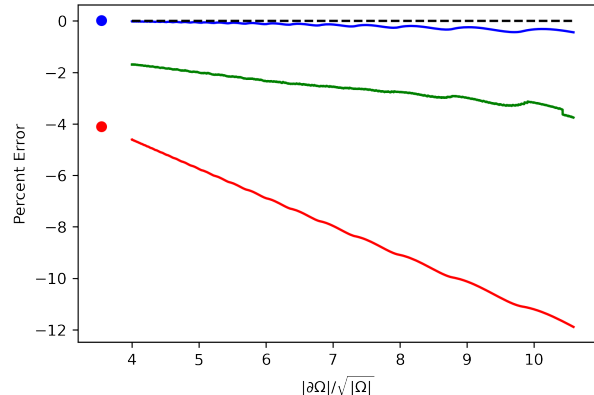


FIG. 4. Red is TF, green is TF on the exact density, and blue is ncTF, for a range of rectangular boxes (continuous) and for a circular cavity (discrete) at  $N = 1000$ . The dimensionless  $|\partial\Omega|/\sqrt{|\Omega|}$  is proportional to  $B$  (Tab. III) and equals  $2\sqrt{\pi}$  for a circle and 4 for a square (see Secs S6 and S7).

Neither of these examples fit in Tab. III, because in both cases the leading correction is zero.

We have given general formulas for  $\Delta N$  in 1D and for any cavity in any dimension, and for specific cases. A more general formula for  $\Delta N$  as a functional of the potential  $v(\mathbf{r})$  would be very powerful and could come from a more general version of the Weyl asymptotics (6). Some relevant asymptotics have been computed for smooth potentials in [47, 48], and the large body of work on the Scott correction, which corresponds to the Coulomb case, is discussed in [49]. It is natural to expect a formula involving a phase space integral, in the spirit of [30].

*Interacting electrons:* In practical applications of DFT, electrons are subject to Coulomb repulsion. In this many-body problem, there is a very specific semiclassical limit of all (non-relativistic) matter, in which the one-body potential is scaled along with  $N$ . In the special case of neutral atoms, this corresponds to simply keeping  $Z = N$ , where  $Z$  is the number of protons in the nucleus.

Over many decades, the asymptotic expansion for neutral atoms was derived:

$$E(N) = -c_0N^{7/3} + N^2/2 - c_2N^{5/3} + \dots,$$

where  $c_0 = 0.769745\dots$  and  $c_2 = 0.269900\dots$  [12, 24, 50] and orbitals are doubly occupied. Here, TF theory (including the Hartree approximation for the electron-

$d$	Example	Potential	$p$	$A$	$B$	$q$
1	interval of length $ \Omega $	0 on $(0,  \Omega )$ and $+\infty$ elsewhere	3	$\frac{\pi^2}{6 \Omega ^2}$	$\frac{1}{2}$	$\frac{d-1}{d}$
1	half harmonic oscillator of frequency $\omega$	$\frac{1}{2}\omega x^2$ on $(0, \infty)$ and $+\infty$ elsewhere	2	$\omega$	$\frac{1}{4}$	$\frac{d-1}{d}$
1	half linear well of strength $F$	$Fx$ on $(0, \infty)$ and $+\infty$ elsewhere	$\frac{5}{3}$	$\frac{(3\pi F)^{2/3}}{2}$	$\frac{1}{4}$	$\frac{d-1}{d}$
2	cavity of area $ \Omega $ and perimeter $ \partial\Omega $	0 on $\Omega \subset \mathbb{R}^2$ and $+\infty$ elsewhere	2	$\frac{\pi}{ \Omega }$	$\frac{ \partial\Omega }{3\sqrt{ \Omega }\pi}$	$\frac{d-1}{d}$
2	quarter harmonic oscillator of frequency $\omega$	$\frac{1}{2}\omega r^2$ on $(0, \infty) \times (0, \infty)$ and $+\infty$ elsewhere	$\frac{3}{2}$	$\frac{4\sqrt{2}}{3}\omega$	$\frac{1}{2\sqrt{2}}$	$\frac{d-1}{d}$
3	cavity of volume $ \Omega $ and surface area $ \partial\Omega $	0 on $\Omega \subset \mathbb{R}^3$ and $+\infty$ elsewhere	$\frac{5}{3}$	$\frac{3(6\pi^2)^{2/3}}{10 \Omega ^{2/3}}$	$\frac{(36\pi)^{1/3} \partial\Omega }{32 \Omega ^{2/3}}$	$\frac{d-1}{d}$
3	Int. Coulomb, $Z = N$	$-\frac{Z}{r}$ on $\mathbb{R}^3 \setminus \{0\}$ , $Z = N$	$\frac{7}{3}$	$-c_0$	$-\frac{3^{2/3}}{14c_0}$	$\frac{d-1}{d}$
3	Non-int. Coulomb, $Z = N$	$-\frac{Z}{r}$ on $\mathbb{R}^3 \setminus \{0\}$ , $Z = N$	$\frac{7}{3}$	$-\frac{3^{1/3}}{2}$	$-\frac{3^{2/3}}{14}$	$\frac{d-1}{d}$
3	Non-int. Coulomb, $Z$ fixed	$-\frac{Z}{r}$ on $\mathbb{R}^3 \setminus \{0\}$	$\frac{1}{3}$	$-\frac{3^{1/3}}{2}$	$-\frac{3^{2/3}}{2}$	$\frac{d-1}{d}$

TABLE III. Constants in Eq. 7. The 1D results are from Eq. (5), those for cavities from Weyl asymptotics, Eq. (6). The quarter harmonic (Sections S4 and S5) and Coulomb (Eq.(9)) results come from explicit formulas for eigenvalues.

electron repulsion) yields precisely the first term alone, while the second is the Scott correction [12, 24, 51]. Setting  $\Delta N = -3(14c_0)^{-1}N^{2/3}$  recovers the Scott correction, yielding the results in Table IV. The asymptotic expansion of  $\tilde{E}_{\text{nc}}$  yields a correction with  $\tilde{c}_2 = 5/(28c_0) = 0.232\dots$ , within 15% of the correct value.

			Percent errors	
Atom	$N$	$E(N)$	$\tilde{E}(N)$	$\tilde{E}_{\text{nc}}(N)$
He	2	-2.904	-33	26
Ne	10	-128.9	-28	7
Ar	18	-527.6	-24	5
Kr	36	-2754	-19	2.8
Xe	54	-7235	-17	2.1
Rn	86	-21870	-15	1.5

TABLE IV. Energies and percent errors for TF and ncTF for nonrelativistic noble gases. For  $N \geq 10$ ,  $E(N)$  obtained by adding exchange-only energies from Table 4.6 of [52] and acGGA+ correlation corrections from Table I of [53]; (correlation is unimportant, being less than a 0.1 per electron).

*The Bohr atom:* We can relate the interacting case above back to our non-interacting examples. The Bohr atom [12, 54, 55] consists of non-interacting fermions (singly) occupying hydrogenic orbitals. If the first  $k$  shells are filled,  $N = 1^2 + 2^2 + \dots + k^2$ , and  $k(N)$  is

the inverse function, then

$$E(N) = -\frac{Z^2}{2}k(N) = -\frac{Z^2}{2}\left((3N)^{1/3} - \frac{1}{2} + \dots\right) \quad (9)$$

We consider two distinct expansions. In the first,  $Z = 1$  and  $N \gg 1$ , as in all our non-interacting examples. In the second,  $Z = N \gg 1$ , as for interacting examples. In Fig. 5 (and Tab. S2), both significantly improve over simple TF, but the latter is more accurate, even than the Scott correction itself.

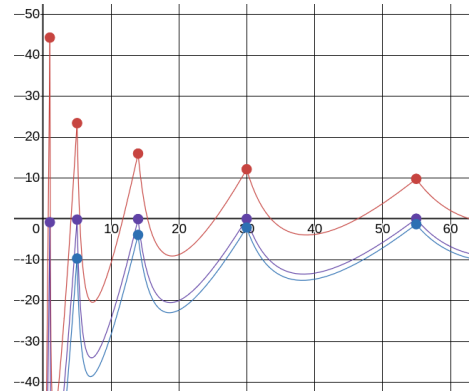


FIG. 5. Percent errors in Bohr atom energies for TF (red), ncTF with  $Z$  fixed (blue), and ncTF with  $Z = N$  (purple). See Section S8 and Table S2.

$N$	$ E_{\text{EXX}}(N) $	$ E_{\text{x}}^{\text{LDA}}(N) $	$ E_{\text{x}}^{\text{PBE}}(N) $	$ E_{\text{nc}}^{\text{LDA}}(N) $
2	1.026	0.862 (16%)	1.005 (2%)	0.978 (5%)
10	12.10	10.97 (9%)	12.03 (0.6%)	11.82 (2%)
18	30.18	27.81 (8%)	29.98 (0.64%)	29.59 (2%)
36	93.83	88.53 (6%)	93.38 (0.5%)	93.03 (0.9%)
54	179.1	170.5 (5%)	178.2 (0.5%)	178.1 (0.5%)
86	387.5	372.9 (4%)	385.9 (0.4%)	387.0 (0.1%)

TABLE V. EXX( $N$ ) is the exact exchange energy,  $E_{\text{x}}^{\text{LDA}}(N)$  the LDA exchange energy,  $E_{\text{x}}^{\text{PBE}}(N)$  the PBE exchange energy, and  $E_{\text{nc}}^{\text{LDA}}(N)$  the normalization-corrected LDA. The first three were obtained from [53].

*Exchange-correlation(XC):* The KS scheme approximates only a small portion of the energy, the XC energy. The simplest approximation is LDAX, the local density approximation for exchange [56–58], which underestimates its magnitude [59]. It uses the exchange energy density of electrons in an infinite box, analogously to the TF calculation for Fig. 1. We take an optimistic leap and imagine that the same forms of Table III apply to LDAX, and simply multiply the density by a factor  $1 + \Delta N/N$ , with  $\Delta N = BN^{2/3}$ . This yields

$$E_{\text{x}}^{\text{LDA}}(\text{NC}) = (1 + B/N^{1/3})^{4/3} E_{\text{x}}^{\text{LDA}}. \quad (10)$$

Choosing  $B = 0.125$  by eye, we find the remarkable improvements shown in Table V for the noble gas atoms, mirroring those for the total energy. The work of [29] *derives* the exact same form for the exchange asymptotics in a 3D box, with  $B \approx 0.47$  (see Section S9), consistent with our guess. Their kinetic energy calculation agrees with our formulas, and also yields a bulk density of  $N + \Delta N$  per unit volume, just as in our examples.

*Outlook:* For a one-dimensional box, one can compute  $\Delta N$  by eye from Fig. 1 by making the straight line of the approximate density go through the middle of the oscillations of the exact density. In less obvious cases, the practicality of normalization corrections will ultimately rely on more robust formulas for  $\Delta N$  as a functional of the potential. The above derivations based on WKB and Weyl asymptotics are special cases of semiclassical asymptotics, which admit many general formulations [38, 60–62]. Work deriving  $\Delta N$  in a universal way from semiclassical trace formulas [47, 48], building on the phase space point of view of [30, 34], is ongoing. Our work emphasizes the need for results with open boundaries rather than cavities. Such results could lead to improvements in accuracy for orbital-free DFT calculations, which scale linearly in  $N$ , avoiding the cubic-in- $N$  calculation of Kohn–Sham orbitals [6]. For applications to solids, these results should generalize to periodic boundary conditions.

The density with  $\Delta N$  extra electrons is not the true density of the system; it is a device guaranteeing more

accurate energetics by improving asymptotics. In principle, one could construct a correction to the TF density functional whose optimal density reproduces these energetics, by taking the functional derivative of the corrected energy with respect to the potential. In practice, this is a non-trivial operation which likely requires some form of regularization in the vicinity of the boundaries.

In future, there are many variations of our tricks that could be applied to the XC functional in a KS calculation, not just the one tried here. Our analysis is also relevant to improving *density-corrected DFT* (DC-DFT), a simple method that has become popular [13–15], where the self-consistent density is replaced by (a proxy for) the exact density. DC-DFT has proven successful in many applications, including ions in solution [63] and the phase diagram of water [64]. But we have shown that a normalization correction of an approximate density can be more accurate than evaluation on the exact density. Our correction is also much easier to implement, not just in this example but in every case we have considered.

*Acknowledgments:* K.D. was supported by NSF Award No. DMS-1708511 and by a Simons Foundation Collaboration Grant for Mathematicians. W.M. and A.W. were supported by NSF Award No. CHE-2306011. K.J.D. would like to thank UCI’s Chancellors Postdoctoral Fellowship Program and in particular Prof. Dr. Feizal Wafar for his support as a sponsor. K.B. was supported by the NSF Award No. CHE-2154371. Thanks also to Hamid Hezari and Antoine Prouff for helpful discussions, and to Vienna Cafe for warm hospitality. K.B. also thanks Gero Friesecke, and Thiago Carvalho Corso, and the Mathematisches Forschungsinstitut Oberwolfach for hospitality.

- 
- [1] J. Austen, *Pride and Prejudice* (T. Egerton, Whitehall, 1813).
  - [2] P. Hohenberg and W. Kohn, Inhomogeneous electron gas, *Phys. Rev.* **136**, B 864 (1964).
  - [3] W. Kohn and L. J. Sham, Self-consistent equations including exchange and correlation effects, *Phys. Rev.* **140**, A 1133 (1965).
  - [4] M. Del Ben, O. Schütt, T. Wentz, P. Messmer, J. Hutter, and J. VandeVondele, Enabling simulation at the fifth rung of dft: Large scale rpa calculations with excellent time to solution, *Computer Physics Communications* **187**, 120 (2015).
  - [5] A. Wasserman and M. Pavanello, Quantum embedding electronic structure methods, *International Journal of Quantum Chemistry* **120**, e26495 (2020), <https://onlinelibrary.wiley.com/doi/pdf/10.1002/qua.26495>.
  - [6] W. Mi, K. Luo, S. B. Trickey, and M. Pavanello, Orbital-free density functional theory: An attractive electronic structure method for large-scale first-principles simulations, *Chemical Reviews* **123**, 12039–12104 (2023).
  - [7] W. Dawson, A. Degomme, M. Stella, T. Nakajima, L. E. Ratcliff, and L. Genovese, Density functional the-



- ory calculations of large systems: Interplay between fragments, observables, and computational complexity, *WIREs Computational Molecular Science* **12**, e1574 (2022).
- [8] D. J. Cole and N. D. M. Hine, Applications of large-scale density functional theory in biology, *Journal of Physics: Condensed Matter* **28**, 393001 (2016).
- [9] O. C. Adekoya, G. J. Adekoya, E. R. Sadiku, Y. Hamam, and S. S. Ray, Application of dft calculations in designing polymer-based drug delivery systems: An overview, *Pharmaceutics* **14**, 1972 (2022).
- [10] M. K. Horton, S. Dwaraknath, and K. A. Persson, Promises and perils of computational materials databases, *Nature Computational Science* **1**, 3–5 (2021).
- [11] M. V. Berry and K. Burke, Exact and approximate energy sums in potential wells, *Journal of Physics A: Mathematical and Theoretical* **53**, 095203 (2020).
- [12] P. Okun and K. Burke, Semiclassics: The hidden theory behind the success of dft, in *Density Functionals for Many-Particle Systems* (WORLD SCIENTIFIC, 2023) p. 179–249.
- [13] E. Sim, S. Song, S. Vuckovic, and K. Burke, Improving results by improving densities: Density-corrected density functional theory, *Journal of the American Chemical Society* **144**, 6625 (2022), pMID: 35380807, <https://doi.org/10.1021/jacs.1c11506>.
- [14] S. Vuckovic, S. Song, J. Kozłowski, E. Sim, and K. Burke, Density functional analysis: The theory of density-corrected dft, *Journal of chemical theory and computation* **15**, 6636 (2019).
- [15] S. Song, S. Vuckovic, E. Sim, and K. Burke, Density-corrected dft explained: Questions and answers, *Journal of Chemical Theory and Computation* **18**, 817 (2022), pMID: 35048707, <https://doi.org/10.1021/acs.jctc.1c01045>.
- [16] M.-C. Kim, E. Sim, and K. Burke, Understanding and reducing errors in density functional calculations, *Phys. Rev. Lett.* **111**, 073003 (2013).
- [17] P. Okun, A. C. Cancio, and K. Burke, Orbital-free potential functionals with submillihartree errors for single-well slabs, *Physical Review B* **109**, 10.1103/physrevb.109.195156 (2024).
- [18] N. Argaman, J. Redd, A. C. Cancio, and K. Burke, Leading correction to the local density approximation for exchange in large- $z$  atoms, *Phys. Rev. Lett.* **129**, 153001 (2022).
- [19] P. Elliott, A. Cangì, S. Pittalis, E. K. U. Gross, and K. Burke, Almost exact exchange at almost no computational cost in electronic structure, *Physical Review A* **92**, 10.1103/physreva.92.022513 (2015).
- [20] L. A. Constantin, E. Fabiano, S. Laricchia, and F. Della Sala, Semiclassical neutral atom as a reference system in density functional theory, *Physical Review Letters* **106**, 10.1103/physrevlett.106.186406 (2011).
- [21] R. F. Ribeiro, D. Lee, A. Cangì, P. Elliott, and K. Burke, Corrections to thomas-fermi densities at turning points and beyond, *Physical Review Letters* **114**, 10.1103/physrevlett.114.050401 (2015).
- [22] L. H. Thomas, The calculation of atomic fields, *Mathematical Proceedings of the Cambridge Philosophical Society* **23**, 542 (1927).
- [23] E. Fermi, Un metodo statistico per la determinazione di alcune proprietà dell'atomo, *Accademia Nazionale dei Lincei* **6**, 602 (1927).
- [24] J. Scott, Lxxxii. the binding energy of the thomas-fermi atom, *The London, Edinburgh, and Dublin Philosophical Magazine and Journal of Science* **43**, 859–867 (1952).
- [25] A. Candel and L. Conlon, *Foliations, Volume 1*, Graduate studies in mathematics (American Mathematical Society, Providence, RI, 1999).
- [26] E. H. Lieb and B. Simon, Thomas-fermi theory revisited, *Physical Review Letters* **31**, 681 (1973).
- [27] E. H. Lieb, Thomas-fermi and related theories of atoms and molecules, *Rev. Mod. Phys.* **53**, 603 (1981).
- [28] C. M. Bender and S. A. Orszag, *Advanced mathematical methods for scientists and engineers I* (Springer, New York, NY, 1999).
- [29] T. C. Corso and G. Friesecke, Next-order correction to the dirac exchange energy of the free electron gas in the thermodynamic limit and generalized gradient approximations, *Journal of Mathematical Physics* **65**, 081902 (2024).
- [30] N. H. March and J. S. Plaskett, The relation between the wentzel-kramers-brillouin and the thomas-fermi approximations, *Proceedings of the Royal Society of London. Series A. Mathematical and Physical Sciences* **235**, 419–431 (1956).
- [31] H. Friedrich, *Theoretical Atomic Physics* (Springer International Publishing, 2017).
- [32] E. C. Titchmarsh, On the asymptotic distribution of eigenvalues, *The Quarterly Journal of Mathematics* **5**, 228–240 (1954).
- [33] V. P. Maslov and M. V. Fedoriuk, *Semi-classical approximation in quantum mechanics*, 1981st ed., *Mathematical Physics and Applied Mathematics* (Kluwer Academic, Dordrecht, Netherlands, 1981).
- [34] A. Cangì, D. Lee, P. Elliott, and K. Burke, Leading corrections to local approximations, *Phys. Rev. B* **81**, 235128 (2010).
- [35] K. Burke, Deriving approximate functionals with asymptotics, *Faraday Discussions* **224**, 98–125 (2020).
- [36] H. Weyl, Ueber die asymptotische verteilung der eigenwerte, *Nachrichten von der Gesellschaft der Wissenschaften zu Göttingen, Mathematisch-Physikalische Klasse* **1911**, 110 (1911).
- [37] H. Weyl, Über die randwertaufgabe der strahlungstheorie und asymptotische spektralgesetze., *crl* **1913**, 177–202 (1913).
- [38] V. Ivrii, 100 years of weyl's law, *Bulletin of Mathematical Sciences* **6**, 379 (2016).
- [39] E. M. Harrell II, L. Provenzano, and J. Stubbe, Complementary asymptotically sharp estimates for eigenvalue means of laplacians, *International Mathematics Research Notices* **2021**, 8405–8450 (2019).
- [40] W. Arendt, R. Nittka, W. Peter, and F. Steiner, Weyl's law: Spectral properties of the laplacian in mathematics and physics (2009).
- [41] J. J. Duistermaat and V. W. Guillemin, The spectrum of positive elliptic operators and periodic bicharacteristics, *Inventiones Mathematicae* **29**, 39–79 (1975).
- [42] V. Y. Ivrii, Second term of the spectral asymptotic expansion of the laplace - beltrami operator on manifolds with boundary, *Functional Analysis and Its Applications* **14**, 98–106 (1980).
- [43] R. L. Frank and L. Geisinger, Two-term spectral asymptotics for the dirichlet laplacian on a bounded domain, in *Mathematical Results in Quantum Physics* (World Scien-

- tific, 2011).
- [44] R. L. Frank and L. Geisinger, Semi-classical analysis of the laplace operator with robin boundary conditions, *Bulletin of Mathematical Sciences* **2**, 281–319 (2012).
  - [45] R. L. Frank and S. Larson, Two-term spectral asymptotics for the dirichlet laplacian in a lipschitz domain, *Journal für die reine und angewandte Mathematik (Crelles Journal)* **2020**, 195–228 (2019).
  - [46] R. L. Frank and S. Larson, Riesz means asymptotics for dirichlet and neumann laplacians on lipschitz domains (2024), arXiv:2407.11808 [math.SP].
  - [47] B. Helffer and D. Robert, Riesz means of bound states and semiclassical limit connected with a lieb–thirring’s conjecture, *Asymptotic Analysis* **3**, 91–103 (1990).
  - [48] V. Guillemin and Z. Wang, Semiclassical spectral invariants for schrödinger operators, *Journal of Differential Geometry* **91**, 10.4310/jdg/1343133702 (2012).
  - [49] R. L. Frank, K. Merz, and H. Siedentop, The scott conjecture for large coulomb systems: a review, *Letters in Mathematical Physics* **113**, 10.1007/s11005-023-01631-9 (2023).
  - [50] J. Schwinger, Thomas-fermi model: The second correction, *Physical Review A* **24**, 2353–2361 (1981).
  - [51] J. Schwinger, Thomas-fermi model: The leading correction, *Physical Review A* **22**, 1827–1832 (1980).
  - [52] R. M. D. Eberhard Engel, *Theoretical, Mathematical & Computational Physics* (Springer-Verlag Berlin Heidelberg, Berlin, Heidelberg, 2011).
  - [53] A. Cancio, G. P. Chen, B. T. Krull, and K. Burke, Fitting a round peg into a round hole: Asymptotically correcting the generalized gradient approximation for correlation, *The Journal of Chemical Physics* **149**, 084116 (2018), <https://doi.org/10.1063/1.5021597>.
  - [54] O. J. Heilmann and E. H. Lieb, Electron density near the nucleus of a large atom, *Phys. Rev. A* **52**, 3628 (1995).
  - [55] B.-G. Englert, *Semiclassical Theory of Atoms* (Springer Berlin Heidelberg, 1988).
  - [56] P. A. M. Dirac, Note on exchange phenomena in the thomas atom, *Mathematical Proceedings of the Cambridge Philosophical Society* **26**, 376 (1930).
  - [57] F. Bloch, Bemerkung zur elektronentheorie des ferromagnetismus und der elektrischen leitfähigkeit, *Zeitschrift für Physik* **57**, 545–555 (1929).
  - [58] J. C. Slater, A simplification of the hartree-fock method, *Phys. Rev.* **81**, 385 (1951).
  - [59] H. Eschrig, *The fundamentals of density functional theory*, Teubner Texte Zur Physik (Vieweg+Teubner Verlag, Wiesbaden, Germany, 1996).
  - [60] M. Dimassi and J. Sjöstrand, *Spectral Asymptotics in the Semi-Classical Limit* (Cambridge University Press, 1999).
  - [61] M. Zworski, *Semiclassical Analysis* (American Mathematical Society, 2012).
  - [62] V. Guillemin and S. Sternberg, *Semi-Classical Analysis* (International Press, 2013).
  - [63] M.-C. Kim, E. Sim, and K. Burke, Ions in solution: Density corrected density functional theory (dc-dft), *J. Chem. Phys.* **140**, 18A528 (2014).
  - [64] S. Song, S. Vuckovic, Y. Kim, H. Yu, E. Sim, and K. Burke, Extending density functional theory with near chemical accuracy beyond pure water, *Nature Communications* **14**, 10.1038/s41467-023-36094-y (2023).

# Supplemental Material: Approximate normalizations for approximate density functionals

Adam Clay<sup>1</sup>, Kiril Datchev<sup>1</sup>, Wenlan Miao<sup>2</sup>, Adam Wasserman<sup>2,3</sup>, Kimberly J. Daas<sup>4</sup>, and Kieron Burke<sup>4,5</sup>

<sup>1</sup>*Department of Mathematics, Purdue University, West Lafayette, IN 47907, USA*

<sup>2</sup>*Department of Physics and Astronomy, Purdue University, West Lafayette, IN 47907, USA*

<sup>3</sup>*Department of Chemistry, Purdue University, West Lafayette, IN 47907, USA*

<sup>4</sup>*Department of Chemistry, University of California, Irvine, CA 92697, USA and*

<sup>5</sup>*Department of Physics and Astronomy, University of California, Irvine, CA 92697, USA*

## CONTENTS

S1	Energy expressions of the one-dimensional box . . . . .	1
S2	Derivation of general energy expressions in one dimension . . . . .	2
S3	Energy expressions of the three-dimensional rectangular box . . . . .	4
S4	Energy expressions of the two-dimensional Harmonic Oscillator . . . . .	4
S5	Energy expressions of the two-dimensional quarter Harmonic Oscillator . . . . .	5
S6	Energy expressions of the two-dimensional rectangular box . . . . .	5
S7	Energy expressions of the two-dimensional circular cavity . . . . .	6
S8	Energy expressions for the Bohr atoms . . . . .	7
S9	Normalization correction for LDAX for a 3D Box . . . . .	8
S10	Table S1: Energies of the particle in a box. . . . .	9
S11	Table S2: Energies of the Bohr Atom . . . . .	10
	References . . . . .	10

## S1. ENERGY EXPRESSIONS OF THE ONE-DIMENSIONAL BOX

The exact energy of  $N$  particles in a box of length  $L$  is

$$E(N) = \frac{\pi^2}{6L^2} \left( N^3 + \frac{3}{2}N^2 + \frac{1}{2}N \right).$$

The TF energy in this case is

$$\tilde{E}(N) = \frac{\pi^2}{6L^2} N^3$$

and the normalization corrected energy is

$$\tilde{E}_{\text{nc}}(N) = \frac{\pi^2}{6L^2} \left( N + \frac{1}{2} \right)^3 = \frac{\pi^2}{6L^2} \left( N^3 + \frac{3}{2}N^2 + \frac{3}{4}N + \frac{1}{8} \right).$$

The exact density in the TF energy functional gives,

$$\tilde{E}_{\text{d}}(N) = \frac{4\pi^2}{3L^3} \int_0^L \left( \sum_{n=1}^N \sin^2 \left( \frac{n\pi x}{L} \right) \right)^3 dx = \frac{\pi^2}{3L^3} \int_0^L \left( 2N + 1 - \frac{\sin((2N+1)\pi x/L)}{\sin(\pi x/L)} \right)^3 dx,$$

which simplifies to

$$\tilde{E}_{\text{d}}(N) = \frac{\pi^2}{6L^2} \left( N^3 + \frac{9}{8}N^2 + \frac{3}{8}N \right),$$

as shown in [1] with  $\zeta = 1$ .



*Ionization energies:* The normalization-correction approach also leads to improved accuracy for ionization energies. For example, for  $N$  non-interacting electrons in a one-dimensional box of length  $L$ , the exact ionization energy is

$$I = E(N) - E(N - 1) = \frac{\pi^2}{2L^2} N^2$$

The Thomas-Fermi approximation is

$$\begin{aligned} \tilde{I} &= \tilde{E}(N) - \tilde{E}(N - 1) \\ &= \frac{\pi^2}{2L^2} \left( N^2 - N + \frac{1}{3} \right) \end{aligned} \quad (\text{S1})$$

The linear-in- $N$  error is eliminated by our normalization-correction approach, since:

$$\begin{aligned} \tilde{I}_{\text{nc}} &= \tilde{E}\left(N + \frac{1}{2}\right) - \tilde{E}\left(N - \frac{1}{2}\right) \\ &= \frac{\pi^2}{2L^2} \left( N^2 + \frac{1}{12} \right) \end{aligned} \quad (\text{S2})$$

## S2. DERIVATION OF GENERAL ENERGY EXPRESSIONS IN ONE DIMENSION

To derive Eq. 4, observe that

$$1 - s'(\alpha) = \sum_{j=-\infty}^{\infty} \delta(\alpha - j).$$

Hence

$$E(N) = \sum_{j=1}^N \mathcal{E}(\lambda(j)) = \int_{1/2}^{N+1/2} d\alpha \left( \mathcal{E}(\lambda(\alpha))(1 - s'(\alpha)) \right).$$

Now integrate by parts in the second term to obtain

$$E(N) = \int_{1/2}^{N+1/2} d\alpha \left( \mathcal{E}(\lambda(\alpha)) + \mathcal{E}'(\lambda(\alpha))\lambda'(\alpha)s(\alpha) \right),$$

where we used  $s(1/2) = s(N + 1/2) = 0$ . This is Eq. 4.



FIG. S1. The auxiliary functions  $s$  is in red and  $S$  in blue, where  $S$  is an antiderivative of  $s$ .

Getting from Eq. 4 to Eq. 5 is much more technical. We begin with an outline of the argument. First, we will show that writing

$$\int_{1/2}^{N+1/2} d\alpha \left( \mathcal{E}(\lambda(\alpha)) + \mathcal{E}'(\lambda(\alpha))\lambda'(\alpha)s(\alpha) \right) \approx \int_{1/2}^{N+1/2} d\alpha \mathcal{E}(\lambda(\alpha))$$

is correct because the integral of  $\mathcal{E}'(\lambda(\alpha))\lambda'(\alpha)s(\alpha)$  is two orders smaller than the integral of  $\mathcal{E}(\lambda(\alpha))$ , one order being gained by going from  $\mathcal{E}$  to  $\mathcal{E}'$ , and another order being gained by the oscillations of  $s$ , which are exploited using integration by parts.

Next, we will show that writing

$$\int_{1/2}^{N+1/2} d\alpha \mathcal{E}(\lambda(\alpha)) \approx \int_{1/2}^{N+1/2} d\alpha \mathcal{E}(\alpha - \nu) = \int_{-\nu+1/2}^{N-\nu+1/2} d\lambda \mathcal{E}(\lambda)$$

is correct because  $\lambda(\alpha) - (\alpha - \nu)$  is two orders smaller than  $\lambda(\alpha)$ . Finally, we will deduce Eq. 5 by showing that writing

$$\int_{-\nu+1/2}^{N-\nu+1/2} d\lambda \mathcal{E}(\lambda) \approx \int_0^{N-\nu+1/2} d\lambda \mathcal{E}(\lambda)$$

is correct because the integral from 0 to  $-\nu + 1/2$  is bounded in  $N$ .

To justify these steps we make the following assumptions. Assume:

$$\mathcal{E}(\lambda) = O(\lambda^{p-1}), \quad \mathcal{E}'(\lambda) = O(\lambda^{p-2}), \quad \mathcal{E}''(\lambda) = O(\lambda^{p-3}),$$

$$\lambda(\alpha) = O(\alpha), \quad \lambda'(\alpha) = O(1), \quad \lambda''(\alpha) = O(\alpha^{-1}),$$

$$r(\alpha) = O(\alpha^{-1}), \quad r'(\alpha) = O(\alpha^{-2})$$

$$\mathcal{E}(\lambda)^{-1} = O(\lambda^{1-p}).$$

To bound the second term of Eq. 4, integrate by parts again to get

$$\int_{1/2}^{N+1/2} d\alpha \mathcal{E}'(\lambda(\alpha))\lambda'(\alpha)s(\alpha) = - \int_{1/2}^{N+1/2} d\alpha \left( \mathcal{E}'(\lambda(\alpha))\lambda'(\alpha) \right)' S(\alpha),$$

where  $S(\lambda) = \int_{1/2}^{\lambda} s$ ; note that  $S$  vanishes at all the half-integers.

Then use

$$|(\mathcal{E}''(\lambda(\alpha))\lambda'(\alpha)^2 + \mathcal{E}'(\lambda(\alpha))\lambda''(\alpha))S(\alpha)| = O(\alpha^{p-3}),$$

to get

$$\left| E(N) - \int_{1/2}^{N+1/2} d\alpha \mathcal{E}(\lambda(\alpha)) \right| = O(N^{p-2}).$$

Next, use  $\lambda'(\alpha) = 1 + r'(\alpha)$  to write, assuming that  $\lambda$  is extended from integer to noninteger values so as to be increasing,

$$\int_{1/2}^{N+1/2} d\alpha \mathcal{E}(\lambda(\alpha)) = \int_{1/2-\nu+r(1/2)}^{N+1/2-\nu+r(N+1/2)} \frac{d\lambda \mathcal{E}(\lambda)}{1 + r'(\alpha(\lambda))}.$$

Since

$$\frac{1}{1 + r'(\alpha(\lambda))} = 1 - \frac{r'(\alpha(\lambda))}{1 + r'(\alpha(\lambda))},$$

and  $r'(\alpha(\lambda)) = O(\lambda^{-2})$ , we see that

$$\frac{\mathcal{E}(\lambda)r'(\alpha(\lambda))}{1 + r'(\alpha(\lambda))} = \frac{O(\lambda^{p-1})O(\lambda^{-2})}{1 + O(\lambda^{-2})} = O(\lambda^{p-3}),$$

so that

$$\left| \int_{1/2-\nu+r(1/2)}^{N+1/2-\nu+r(N+1/2)} d\lambda \left( \frac{\mathcal{E}(\lambda)}{1 + r'(\alpha(\lambda))} - \mathcal{E}(\lambda) \right) \right| = O(N^{p-2}).$$

Meanwhile

$$\left| \int_{1/2-\nu+r(1/2)}^{N+1/2-\nu+r(N+1/2)} d\lambda \mathcal{E}(\lambda) - \int_{1/2-\nu+r(1/2)}^{N+1/2-\nu} d\lambda \mathcal{E}(\lambda) \right| = O(N^{p-2}),$$

because the difference is integrating a function of size  $O(N^{p-1})$  over a region of size  $O(N^{-1})$ . Similarly, we can adjust the lower limit:

$$\left| \int_{1/2-\nu+r(1/2)}^{N+1/2-\nu} d\lambda \mathcal{E}(\lambda) - \int_0^{N+1/2-\nu} d\lambda \mathcal{E}(\lambda) \right| = O(1).$$

Putting together these bounds yields

$$\left| E(N) - \int_0^{N+1/2-\nu} d\lambda \mathcal{E}(\lambda) \right| = O(N^{p-2}) + O(1).$$

If  $p > 2$  then the first remainder dominates, and if  $p < 2$  then the second one does.

### S3. ENERGY EXPRESSIONS OF THE THREE-DIMENSIONAL RECTANGULAR BOX

A 3d rectangular box with sides lengths  $L_x$ ,  $L_y$  and  $L_z$  has energy levels

$$E(N) = \sum_{i,j,k}^{E_{ijk} < R(N)^2} \mathcal{E}_{ijk}$$

$$\mathcal{E}_{ijk} = \frac{1}{2} \frac{i^2 \pi^2}{L_x^2} + \frac{1}{2} \frac{j^2 \pi^2}{L_y^2} + \frac{1}{2} \frac{k^2 \pi^2}{L_z^2},$$

where  $R(N)$  is the radius of the quantum number space:  $R(N) = (2^3 N / (L_x L_y L_z))^{1/3}$ . The TF energy is

$$\tilde{E}(N) = \frac{3(6\pi^2)^{2/3}}{10|\Omega|^{2/3}} N^{5/3}$$

while the normalization corrected energy is

$$\tilde{E}_{\text{nc}}(N) = \frac{3(6\pi^2)^{2/3}}{10|\Omega|^{2/3}} \left( N + \frac{(36\pi^{1/3})|\partial\Omega|}{32|\Omega|^{2/3}} N^{2/3} \right)^{5/3}.$$

The TF energy on the exact density is

$$\tilde{E}_{\text{d}}(N) = \frac{24(6\pi^2)^{2/3}}{10|\Omega|} \iint \sum_{i,j,k}^{E_{ijk} < R(N)^2} \left( \sin^2 \left( \frac{i\pi x}{L_x} \right) \sin^2 \left( \frac{j\pi y}{L_y} \right) \sin^2 \left( \frac{k\pi z}{L_z} \right) \right)^{5/3} dx dy dz.$$

The energies and percentage errors from  $N = 1$  to  $N = 1000$  can be found in 3d-box.txt.

### S4. ENERGY EXPRESSIONS OF THE TWO-DIMENSIONAL HARMONIC OSCILLATOR

For the two-dimensional harmonic oscillator with frequency  $\omega$  the exact energy expression is given in Eq. 8 of the main text. To derive it, let  $H = -(1/2)\nabla^2 + \frac{1}{2}\omega^2 r^2$ . The energy levels are

$$\mathcal{E}_{m,n} = (m + n + 1)\omega,$$

where  $m$  and  $n$  are the quantum numbers corresponding to the  $x$  and  $y$  space coordinates. Hence the energy level  $i\omega$  has degeneracy  $i$ . If we have  $N$  particles filling up energy levels up to the  $N_\ell$ th level, then

$$N = \sum_{i=1}^{N_\ell} i = \frac{1}{2}(N_\ell^2 + N_\ell), \quad \text{or} \quad N_\ell = \frac{1}{2}\sqrt{8N + 1} - \frac{1}{2}.$$

The total energy is

$$E(N) = \sum_{i=1}^{N_\ell} i \cdot i\omega = N_\ell(N_\ell + 1)(2N_\ell + 1)\frac{\omega}{6} = \frac{\omega}{3}N\sqrt{8N+1} = \frac{2\sqrt{2}}{3}\omega N^{3/2} + \frac{1}{12\sqrt{2}}\omega N^{1/2} + \dots,$$

the TF energy is

$$\tilde{E}(N) = \frac{2\sqrt{2}}{3}\omega N^{3/2},$$

and the normalization corrected energy is

$$\tilde{E}_{\text{nc}}(N) = \frac{2\sqrt{2}}{3}\omega\left(N + \frac{1}{24}\right)^{3/2}.$$

## S5. ENERGY EXPRESSIONS OF THE TWO-DIMENSIONAL QUARTER HARMONIC OSCILLATOR

The quarter harmonic oscillator is similar. In that case, the energy levels are

$$\mathcal{E}_{m,n} = (2m + 2n + 3)\omega.$$

which means the energy level  $(2i + 1)\omega$  has degeneracy  $i$ . If we have  $N$  particles filling up energy levels up to the  $N_\ell$ th level, then

$$N = \sum_{i=1}^{N_\ell} i = \frac{1}{2}(N_\ell^2 + N_\ell), \quad \text{or} \quad N_\ell = \frac{1}{2}\sqrt{8N+1} - \frac{1}{2}.$$

The total energy is

$$E(N) = \sum_{i=1}^{N_\ell} i \cdot (2i + 1)\omega = N_\ell(N_\ell + 1)(4N_\ell + 5)\frac{\omega}{6} = N\left(2\sqrt{8N+1} + 3\right)\frac{\omega}{3} = \frac{4\sqrt{2}}{3}\omega N^{3/2} + \omega N + \dots,$$

the TF energy is

$$\tilde{E}(N) = \frac{4\sqrt{2}}{3}\omega N^{3/2},$$

and the normalization corrected energy is

$$\tilde{E}_{\text{nc}}(N) = \frac{4\sqrt{2}}{3}\omega\left(N + \frac{1}{2\sqrt{2}}N^{1/2}\right)^{3/2}.$$

## S6. ENERGY EXPRESSIONS OF THE TWO-DIMENSIONAL RECTANGULAR BOX

A rectangular box with side lengths  $L_x$  and  $L_y$  has energy levels

$$\mathcal{E}_{i,j} = \frac{1}{2}\frac{i^2\pi^2}{L_x^2} + \frac{1}{2}\frac{j^2\pi^2}{L_y^2},$$

where  $i$  and  $j$  are the quantum numbers corresponding to the sides of length  $L_x$  and  $L_y$  respectively. The exact energy is given by,

$$E(N) = \sum_{i,j}^{\mathcal{E}_{i,j} < R(N)^2} \mathcal{E}_{i,j},$$

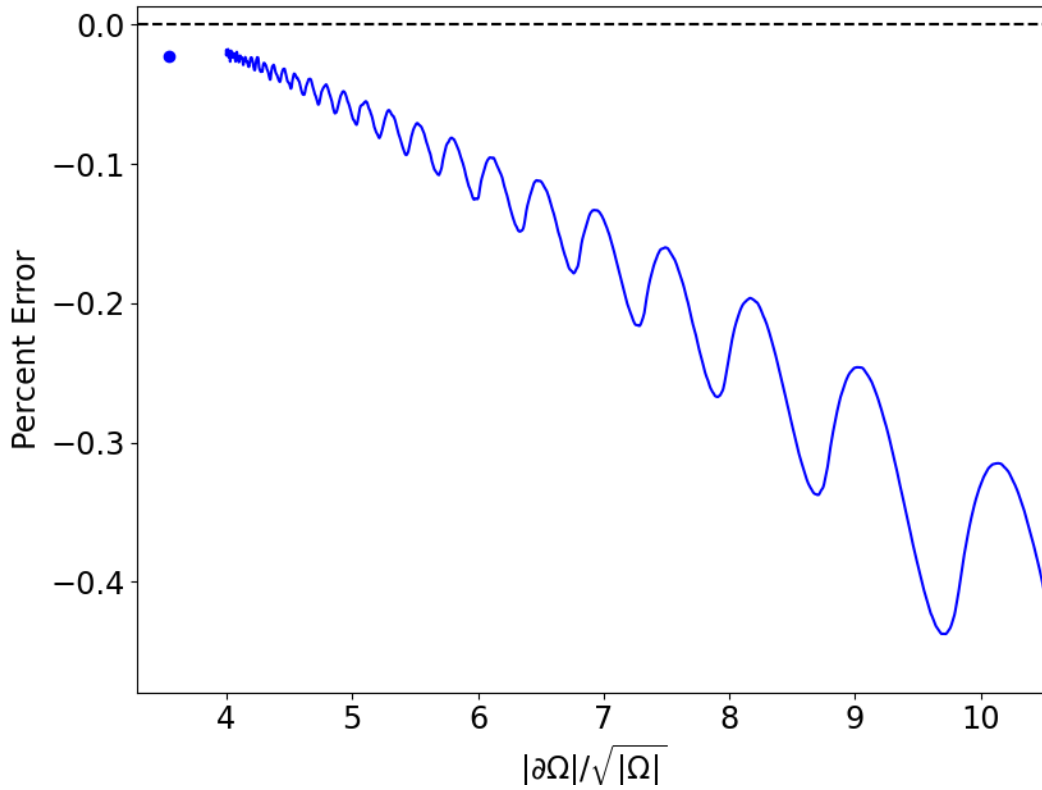


FIG. S2. A zoom of Figure 4.

where  $R(N)$  is the radius of the quantum number space:  $R(N) = (2^2 N / (L_x L_y))^{1/2}$ . The TF energy is

$$\tilde{E}(N) = AN^p = \frac{\pi}{|\Omega|} N^2,$$

and the normalization corrected energy is

$$\tilde{E}_{\text{nc}}(N) = \frac{\pi}{|\Omega|} \left( N + \frac{|\partial\Omega|}{3\sqrt{|\Omega|}\pi} N^{1/2} \right)^2,$$

because the Weyl asymptotic formula is

$$E(N) = \frac{\pi}{A} N^2 + \frac{2\sqrt{\pi}|\partial\Omega|}{3|\Omega|^{3/2}} N^{3/2} + \dots$$

The TF energy with the exact density can be written as

$$\tilde{E}_d(N) = \frac{4\pi}{|\Omega|} \iint \sum_{i,j}^{E_{i,j} < R(N)^2} \left( \sin^2 \left( \frac{i\pi x}{L_x} \right) \sin^2 \left( \frac{j\pi y}{L_y} \right) \right)^2 dx dy.$$

. The energies and percentage errors for  $N = 1000$  can be found in 2d\_box.txt.

## S7. ENERGY EXPRESSIONS OF THE TWO-DIMENSIONAL CIRCULAR CAVITY

Separation of variables yields the radial equation

$$-\frac{1}{2}u''(r) - \frac{1}{2r}u'(r) + \frac{\ell^2}{2r^2}u(r) = \mathcal{E}u(r),$$



where  $\ell = 0, 1, 2, \dots$  is the angular momentum. Solutions which are regular at  $r = 0$  are given in terms of Bessel functions by  $u(r) = J_\ell(\sqrt{2\mathcal{E}}r)$ . Imposing the boundary condition  $u(R) = 0$  tells us that, if the cavity has radius  $R$ , then  $\sqrt{2\mathcal{E}}R$  must be a zero of the Bessel function  $J_\ell$ . In other words, the energy levels are

$$\mathcal{E}_{\ell,n} = \frac{j_{\ell,n}^2}{2R^2},$$

where  $j_{\ell,n}$  is the  $n$ th zero of  $J_\ell$ . Thus, if  $R = 1$ , then the first twelve energy levels in order are

$$\mathcal{E}_{0,1} \approx 2.89, \quad \mathcal{E}_{1,1} \approx 7.34, \quad \mathcal{E}_{2,1} \approx 13.19, \quad \mathcal{E}_{0,2} \approx 15.24, \quad \mathcal{E}_{3,1} \approx 20.35, \quad \mathcal{E}_{1,2} \approx 24.61,$$

$$\mathcal{E}_{4,1} \approx 28.79, \quad \mathcal{E}_{2,2} \approx 35.42, \quad \mathcal{E}_{0,3} \approx 37.43, \quad \mathcal{E}_{5,1} \approx 38.47, \quad \mathcal{E}_{3,2} \approx 47.64, \quad \mathcal{E}_{6,1} \approx 49.36,$$

Energy levels with  $\ell = 0$  are nondegenerate, because the angular wave function is constant, while those with  $\ell \geq 1$  are doubly degenerate, because the angular wave function is a combination of  $\cos(\ell\theta)$  and  $\sin(\ell\theta)$ ; there are no further degeneracies because  $j_{\ell,n} \neq j_{\ell',n'}$  when  $(\ell, n) \neq (\ell', n')$  [2, §15.28]. The energies and percentage errors for  $N = 1000$  can be found in 2d\_box.txt. The exact density is given in terms of Bessel functions by

$$n(\mathbf{r}) = \frac{1}{\pi} \sum_{\{m,k\} \in \text{lowest } N} c_{mk} [J_m(j_{mk}r)]^2.$$

with

$$c_{mk} = \frac{g_{mk}}{[J_{m-1}(j_{mk})]^2},$$

where  $g_{mk}$  are the occupation numbers for each state:

$$g_{mk} = \begin{cases} 1, & m = 0, \\ 2, & m \geq 1. \end{cases}$$

The TF density is

$$n^{\text{TF}}(\mathbf{r}) = \frac{N}{\pi},$$

and the normalization corrected density is

$$n_{\text{nc}}^{\text{TF}}(\mathbf{r}) = \frac{N + \sqrt{N}}{\pi}.$$

The densities on a grid from  $r = 0$  to  $r = 1$  can be found in 2d\_cavity.txt.

## S8. ENERGY EXPRESSIONS FOR THE BOHR ATOMS

The exact energies for the closed shell atoms are

$$E(N) = -\frac{N^2}{4} \left( A(N) - 1 + \frac{1}{3A(N)} \right)$$

with  $A(N)^3 = 12N \left( 1 - \sqrt{1 - (3888N^2)^{-1}} \right)$ , which is a version of the formula from [3], modified for singly occupied orbitals. For open shell atoms the formula is,

$$E(N) = -\frac{N^2}{2} \sum_{n=1}^N f_n$$

where  $f_n$  is the  $n$ th element of the series of  $\frac{1}{n^2}$  where each member is repeated  $n^2$  times, i.e.

$$1, \frac{1}{4}, \frac{1}{4}, \frac{1}{4}, \frac{1}{4}, \frac{1}{9}, \dots, \frac{1}{9}, \frac{1}{16}, \dots, \frac{1}{16}, \frac{1}{25}, \dots, \frac{1}{25}, \dots;$$

see [4] for more details. The TF energy is [3, 5],

$$\tilde{E}(N) = -\frac{3^{\frac{1}{3}}}{2} N^{\frac{7}{3}}.$$

If the Scott correction is added, one obtains

$$\tilde{E}_{\text{sc}}(N) = -\frac{3^{\frac{1}{3}}}{2} N^{\frac{7}{3}} + \frac{1}{4} N^2,$$

where again the extra factor  $\frac{1}{2}$  in front of the Scott correction comes from singly occupying the orbitals. The resulting fixed  $Z$  ( $Z = 1$  and  $N \gg 1$ ) normalization corrections are given by

$$\tilde{E}(N) = -\frac{3^{\frac{1}{3}}}{2} \left( N - \frac{3^{\frac{2}{3}}}{2} N^{\frac{2}{3}} \right)^{\frac{7}{3}},$$

whereas for  $N = Z \gg 1$  they can be found via

$$\tilde{E}_{\text{nc}}(N) = -\frac{3^{\frac{1}{3}}}{2} \left( N - \frac{3^{\frac{2}{3}}}{14} N^{\frac{2}{3}} \right)^{\frac{7}{3}}.$$

### S9. NORMALIZATION CORRECTION FOR LDAX FOR A 3D BOX

By Theorem 1.1 of [6],

$$E_x^{LDA}(N) = -c_x \tilde{\rho}^{4/3} |\Omega| L^3 - c_{x,2}^{Dir} \tilde{\rho} |\partial\Omega| L^2 + \dots,$$

where  $c_x = (3/4)(3/\pi)^{1/3}$ ,  $c_{x,2}^{Dir} \approx 0.0767$ ,  $\tilde{\rho} = N/(|\Omega|L^3)$ , and  $L$  is a scaling parameter for the size of the box. Absorbing  $L^3$  into  $|\Omega|$  and  $L^2$  into  $|\partial\Omega|$  yields

$$E_x^{LDA}(N) = -\frac{c_x}{|\Omega|^{1/3}} N^{4/3} - \frac{c_{x,2}^{Dir} |\partial\Omega|}{|\Omega|} N + \dots.$$

Next,

$$-\frac{c_x}{|\Omega|^{1/3}} (N + \Delta N)^{4/3} = -\frac{c_x}{|\Omega|^{1/3}} N^{4/3} - \frac{4c_x}{3|\Omega|^{1/3}} N^{1/3} \Delta N + \dots,$$

Matching the second term on the right side of each equation yields

$$\frac{c_{x,2}^{Dir} |\partial\Omega|}{|\Omega|} N = \frac{4c_x}{3|\Omega|^{1/3}} N^{1/3} \Delta N,$$

or

$$\Delta N = B N^q, \quad B = \frac{3c_{x,2}^{Dir} |\partial\Omega|}{4c_x |\Omega|^{2/3}}, \quad q = \frac{2}{3}.$$

Comparing with Table II, we see that  $q$  is the same, and  $B$  has the same form as for in the corresponding 3D box calculation. Plugging in  $c_x = (3/4)(3/\pi)^{1/3}$ ,  $c_{x,2}^{Dir} \approx 0.0767$ , and  $|\partial\Omega| = 6|\Omega|^{2/3}$  for a cube, yields

$$B = \frac{3c_{x,2}^{Dir} |\partial\Omega|}{4c_x |\Omega|^{2/3}} = 6 \left( \frac{\pi}{3} \right)^{1/3} c_{x,2}^{Dir} \approx 0.47.$$

S10. TABLE S1: ENERGIES OF THE PARTICLE IN A BOX

N	$E(N)$	$\tilde{E}(N)$	$\tilde{E}_d(N)$	$\tilde{E}_{nc}(N) = \tilde{E}(\tilde{N})$
1.	4.93	1.64 (-66.67%)	4.11 (-16.67%)	5.55 (12.5%)
2.	24.7	13.2 (-46.67%)	21.8 (-11.67%)	25.7 (4.17%)
3.	69.1	44.4 (-35.71%)	62.9 (-8.93%)	70.5 (2.08%)
4.	148	105 (-28.89%)	137 (-7.22%)	150 (1.25%)
5.	271	206 (-24.24%)	255 (-6.06%)	274 (0.83%)
6.	449	355 (-20.88%)	426 (-5.22%)	452 (0.6%)
7.	691	564 (-18.33%)	659 (-4.58%)	694 (0.45%)
8.	1007	842 (-16.34%)	966 (-4.08%)	1010 (0.35%)
9.	1406	1199 (-14.74%)	1355 (-3.68%)	1410 (0.28%)
10.	1900	1645 (-13.42%)	1836 (-3.35%)	1904 (0.23%)
11.	2497	2189 (-12.32%)	2420 (-3.08%)	2502 (0.19%)
12.	3208	2842 (-11.38%)	3116 (-2.85%)	3213 (0.16%)
13.	4042	3614 (-10.58%)	3935 (-2.65%)	4047 (0.14%)
14.	5009	4514 (-9.89%)	4885 (-2.47%)	5015 (0.12%)
15.	6119	5552 (-9.27%)	5977 (-2.32%)	6126 (0.1%)
16.	7382	6738 (-8.73%)	7221 (-2.18%)	7389 (0.09%)
17.	8809	8082 (-8.25%)	8627 (-2.06%)	8816 (0.08%)
18.	10407	9593 (-7.82%)	10204 (-1.96%)	10415 (0.07%)
19.	12189	11283 (-7.44%)	11962 (-1.86%)	12197 (0.07%)
20.	14163	13159 (-7.08%)	13912 (-1.77%)	14171 (0.06%)
21.	16339	15234 (-6.77%)	16063 (-1.69%)	16348 (0.05%)
22.	18728	17515 (-6.47%)	18424 (-1.62%)	18737 (0.05%)
23.	21338	20014 (-6.21%)	21007 (-1.55%)	21348 (0.05%)
24.	24181	22740 (-5.96%)	23820 (-1.49%)	24191 (0.04%)
25.	27265	25702 (-5.73%)	26874 (-1.43%)	27275 (0.04%)
26.	30601	28911 (-5.52%)	30178 (-1.38%)	30612 (0.04%)
27.	34198	32377 (-5.32%)	33743 (-1.33%)	34209 (0.03%)
28.	38067	36110 (-5.14%)	37578 (-1.29%)	38079 (0.03%)
29.	42217	40118 (-4.97%)	41692 (-1.24%)	42229 (0.03%)
30.	46659	44413 (-4.81%)	46097 (-1.2%)	46671 (0.03%)

TABLE S1. Table that contains the data of Fig. 1, with the first column being the number of electrons, the second column the exact energy, the third column the TF energy (red line), the fourth the TF energy obtained with the exact density (green line) and lastly the normalization-corrected TF (blue line) for the particle in a box. The percentage errors between the approximations and the exact can be found in between brackets

S11. TABLE S2: ENERGIES OF THE BOHR ATOM

N	$E(N)$	$\tilde{E}(N)$	$\tilde{E}_{\text{sc}}(N)$	$\tilde{E}_Z(N)$	$\tilde{E}_{\text{nc}}(N) = \tilde{E}(\tilde{N})$
1.	-0.500	-0.721 (44.2%)	-0.471 (-5.77%)	0.247 (-149%)	-0.495 (-0.91%)
5.	-25.0	-30.8 (23.3%)	-24.6 (-1.69%)	-22.6 (-9.77%)	-24.9 (-0.26%)
14.	-294	-340 (15.9%)	-291 (-0.80%)	-282 (-4.02%)	-293 (-0.12%)
30.	-1800	-2016 (12.0%)	-1791 (-0.46%)	-1760 (-2.19%)	-1798 (-0.069%)
55.	-7563	-8295 (9.70%)	-7539 (-0.30%)	-7457 (-1.39%)	-7559 (-0.045%)

TABLE S2. Table that contains the data of Fig. 5, with the first column being the number of electrons, the second column the exact energy, the third column the TF energy (red line), the fourth Scott corrected TF energy, the fifth the TF energy with  $Z$  fixed (blue line) and lastly the normalization-corrected TF (purple line) for the Bohr atom. The percentage errors between the approximations and the exact can be found in between brackets.

- 
- [1] P. Elliott, D. Lee, A. Cangi, and K. Burke, Semiclassical origins of density functionals, *Phys. Rev. Lett.* **100**, 256406 (2008).  
[2] G. N. Watson, *A Treatise on the Theory of Bessel Functions* (Cambridge University Press, 1944).  
[3] P. Okun and K. Burke, Semiclassics: The hidden theory behind the success of dft, in *Density Functionals for Many-Particle Systems* (WORLD SCIENTIFIC, 2023) p. 179–249.  
[4] K. Burke, A. Cancio, T. Gould, and S. Pittalis, Locality of correlation in density functional theory, *The Journal of Chemical Physics* **145**, 054112 (2016).  
[5] O. J. Heilmann and E. H. Lieb, Electron density near the nucleus of a large atom, *Phys. Rev. A* **52**, 3628 (1995).  
[6] T. C. Corso and G. Friesecke, Next-order correction to the dirac exchange energy of the free electron gas in the thermodynamic limit and generalized gradient approximations, *Journal of Mathematical Physics* **65**, 081902 (2024).